PERGAMON

Journal of Geodynamics 33 (2002) 143–156

JOURNAL OF
GEODYNAMICS

www.elsevier.com/locate/jgeodyn

Modeling the geomagnetic perturbations produced by ionospheric currents, above and below the ionosphere

A.D. Richmond*

National Center for Atmospheric Research, High Altitude Observatory, Boulder, CO 80307-3000, USA

Abstract

This paper briefly surveys the nature of magnetic perturbations at the ground and at low-Earth-orbit (LEO) altitudes produced by ionospheric and geomagnetic-field-aligned currents, with the aid of representative simulation and empirical models. The equatorial electojet, driven by the eastward daytime ionospheric electric field, strongly affects magnetic perturbations near the magnetic equator. Thermospheric winds also influence low-latitude ionospheric currents, and create significant east–west magnetic perturbations at lower LEO altitudes. At midlatitudes, currents flow not only within the ionosphere but also along geomagnetic field lines above the ionosphere. The latter can produe significant large-scale magnetic perturbations above the ionosphere over large regions of space. The largest magnetic perturbations are produced by electric currents in the auroral zones and the geomagnetic-field-aligned currents that connect the ionosphere with the outer magnetosphere. Above the ionosphere, the high-latitude magnetic perturbations tend to be dominated by toroidal magnetic perturbation fields associated with the field-aligned currents. LEO observations of magnetic perturbations can provide valuable information about the drivers of the ionospheric dynamo, the state of the magnetosphere, and the transfer of energy between the magnetosphere and the ionosphere.

1. Introduction

This paper briefly surveys the nature of magnetic perturbations at the ground and at low Earth orbit (LEO, up to 1000 km altitude) produced by ionospheric and field-aligned currents, with the aid of representative simulation and empirical models. Fig. 1 illustrates the types of currents involved. At high magnetic latitudes, geomagnetic-field-aligned currents flow into and out of the auroral zones, and they are accompanied by strong eastward and westward ionospheric currents

* Tel./fax: +1-303-497-1570.
E-mail address: richmond@ucar.edu (A.D. Richmond).

0264-3707/02/$ - see front matter
PII: S0264-3707(01)00060-6

that comprise the auroral electrojets. These currents are closely coupled with the magnetosphere and the solar wind, and they are highly variable, in response to changing magnetospheric and interplanetary conditions. Some of the high-latitude current leaks to lower latitudes. At middle and low latitudes, global-scale currents exist on the day side of the Earth, driven largely by thermospheric winds that produce ionospheric dynamo action. These are often called the S_q currents (S = solar, q = quiet), or sometimes the S_R currents (R = regular). Part of the S_q current flows along geomagnetic-field lines between the northern and southern magnetic hemispheres, when the dynamo action is asymmetric about the equator. Part of this current also connects into the equatorial electrojet, a relatively intense current flowing in the lower dayside ionosphere along the magnetic equator, where a strong vertical polarization electric field can develop that drives strong eastward Hall current. Except for the geomagnetic-field-aligned current, most of the ionospheric current flows between 90 and 200 km altitude. However, small but measurable cross-field currents can also flow above 200 km both day and night, especially during high solar activity, when the ionospheric conductivity above 200 km is much larger than it is for low solar activity (Takeda and Araki, 1985).

Ground magnetometers readily sense the effects of the auroral electrojets and of the S_q currents. LEO satellite magnetometers also sense these, but additionally sense the effects of the field-aligned currents that surround them. Not shown in Fig. 1 is another current system that has also been inferred from the MAGSAT vector magnetometer at low latitudes (Maeda et al., 1982; Takeda and Maeda, 1983). In the late afternoon and early evening, a meridional current rises

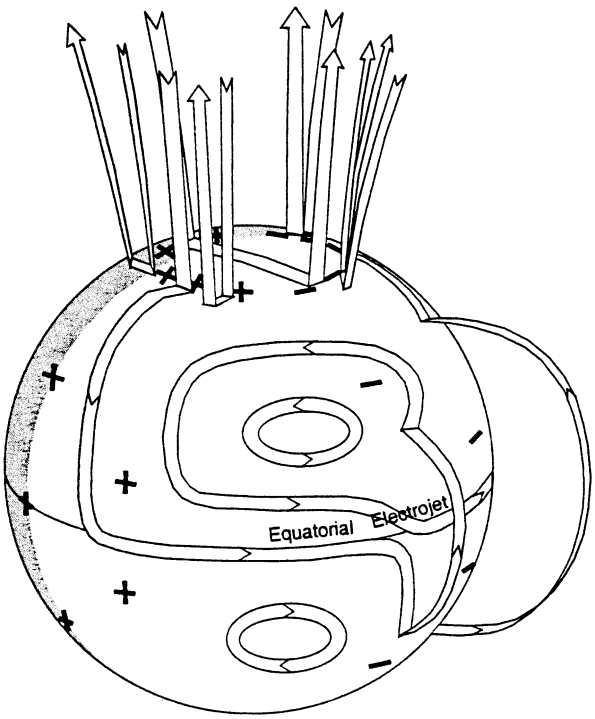

Fig. 1. Schematic of global ionospheric electric currents (ribbons with arrows) and electric potentials (+ and –), viewed from the day side of the Earth. [From Richmond and Thayer (2000). Copyright by the American Geophysical Union.].

over the magnetic equator, up to roughly 400∼km altitude at solar maximum, and flows mainly along geomagnetic field lines northward and southward back down into the lower parts of the ionosphere. As shown in the next section, the direction of this meridional current is in the opposite sense earlier in the day.

2. Equatorial region

At the ground, quiet-day magnetic perturbations under the daytime equatorial electrojet are typically twice as large as those 5° or more away from the magnetic equator, and can exceed 200 nT. The amplitude is about twice as large at the maximum of the solar sunspot cycle as at the minimum, and is usually larger around the equinoxes than at the solstices. Significant variability from day to day is also observed, associated with variability in the global wind systems that drive the ionospheric dynamo and create ionospheric electric fields. The equatorial electrojet is particularly sensitive to the strength of the eastward component of the ionospheric electric field at the magnetic equator.

Two-dimensional models of equatorial ionospheric currents and their associated magnetic perturbations have been presented by Untiedt (1967), Richmond (1973), Fambitakoye et al. (1976), Forbes and Lindzen (1976b), Stening (1985),and Anandarao and Raghavarao (1987). These studies showed that the electrojet perturbation in the magnetic northward magnetic field (H) at the magnetic equator is sensitive primarily to the eastward ionospheric electric field, but that the H perturbation a few degrees away from the equator can be strongly affected by vertical shears in the eastward thermospheric wind between 90 and 200 km. Two simulation results are presented here, using the model of Richmond (1973), to illustrate the structure of the equatorial electrojet currents and magnetic perturbations at various altitudes around midday. The model covers the region 80–400 km altitude and $\pm 10^\circ$ magnetic latitude, assuming a flat Earth and parabolic geomagnetic field lines. The ionospheric conductivities are representative of medium solar activity at noon; the electron-neutral collision frequency is artificially increased by a factor of 4 to simulate the influences of electrojet plasma irregularities, as explained by Gagnepain et al. (1977). The first simulation uses an eastward electric field of 0.5 mV/m, with no thermospheric wind, while the second uses the same eastward electric field but with an eastward wind profile as shown in Fig. 2, assumed to be uniform in latitude and longitude over the modeling region. This wind is westward at high altitudes, in the direction that has generally been observed at low latitudes around midday (Hedin et al., 1991).

Fig. 3 shows, on the left, latitude-height distributions of the eastward electric current density, which is responsible for the north-south and vertical magnetic perturbations seen on the ground as well as at LEO altitudes, and, on the right, the eastward magnetic perturbations within the ionosphere, the contours of which correspond to streamlines of meridional electric current flow: positive eastward magnetic perturbations correspond to counterclockwise current vortices, and negative perturbations to clockwise vortices. At 120 km the current is upward over the equator for both simulations.

The strong eastward equatorial electrojet current is confined within about 95–125 km altitude and $\pm 4^\circ$ magnetic latitude. For weaker (stronger) geomagnetic-field strengths, such as those present at different magnetic longitudes, the altitude of the electrojet current shifts upward

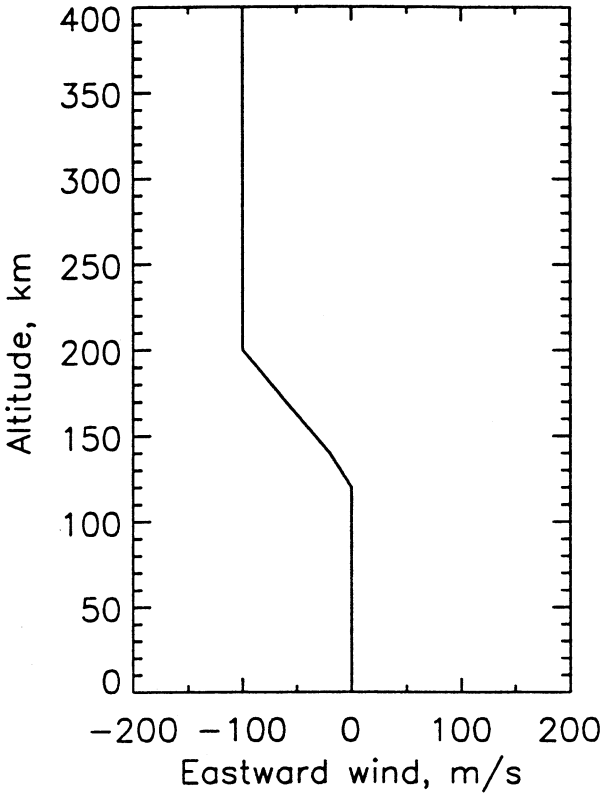

Fig. 2. Vertical distribution of the eastward wind used in modeling equatorial ionospheric electric currents.

(downward) a little. For geomagnetic field lines that have less (more) curvature at the equator than dipole field lines, the electrojet is a little wider (narrower) in geometric north-south distance, but a little narrower (wider) with respect to dip latitude. Beyond about 5° from the equator, it can be seen in Fig. 3 that the eastward current intensity depends significantly on the neutral wind. For the wind profile of Fig.2, the eastward current density below 130 km is significantly enhanced. Relative minima in the height-integrated eastward current density appear around $\pm 5°$.

The eastward magnetic perturbations at higher altitudes are also strongly affected by the presence of the wind, being reversed in direction and usually stronger in amplitude above 150 km with respect to the windless simulation. Note that it is necessary for the wind to vary in height in this model in order to produce changes in the currents. A wind that is constant in height and latitude would produce a uniform upward/poleward polarization electric field that exactly canceled the dynamo field $\mathbf{U}\times\mathbf{B}$, where $\mathbf{U}$ and $\mathbf{B}$ are the wind and magnetic-field vectors, so that the total electric field driving the current would be unchanged.

Fig. 4 shows the magnetic perturbations, calculated from the currents in the simulation that includes winds, at three different altitudes: at the ground, at 200 km, and at 400 km. To calculate the northward (H) and downward (Z) perturbations, the eastward current density is first divided into two components: a "background" component that is independent of latitude and representative of the current density at distant latitudes, and a latitude-dependent electrojet supple-

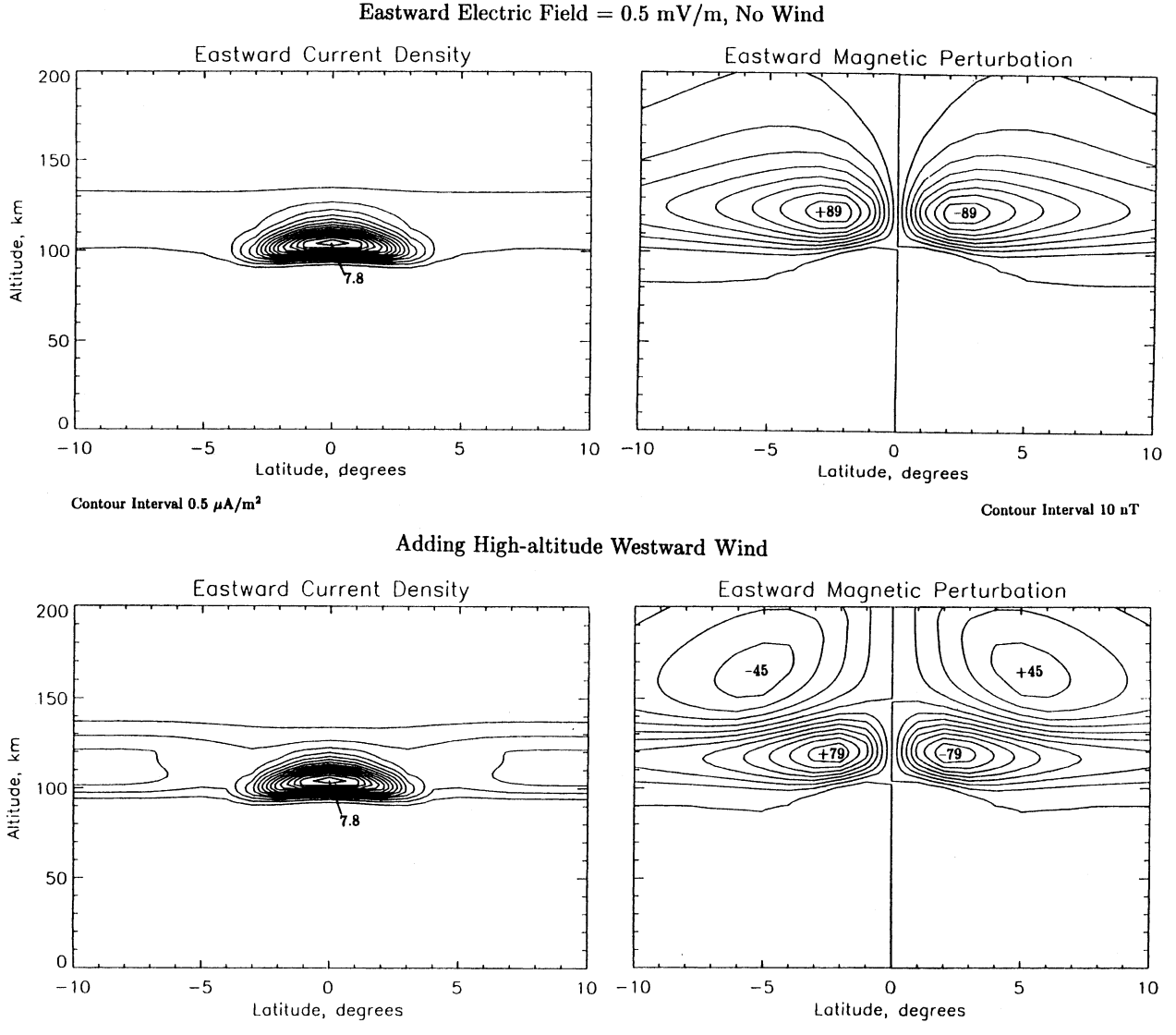

Fig. 3. Distributions of modeled eastward electric current density (left) and eastward magnetic perturbations (right) as a function of magnetic latitude and altitude. Results from two simulations are shown: (top) eastward electric field = 0.5 mV/m, no wind; (bottom) eastward electric field = 0.5 mV/m, latitude-independent wind as shown in Fig. 2. Peak eastward current densities are in $\mu A/m^2$. Peak eastward magnetic perturbations are in nT.

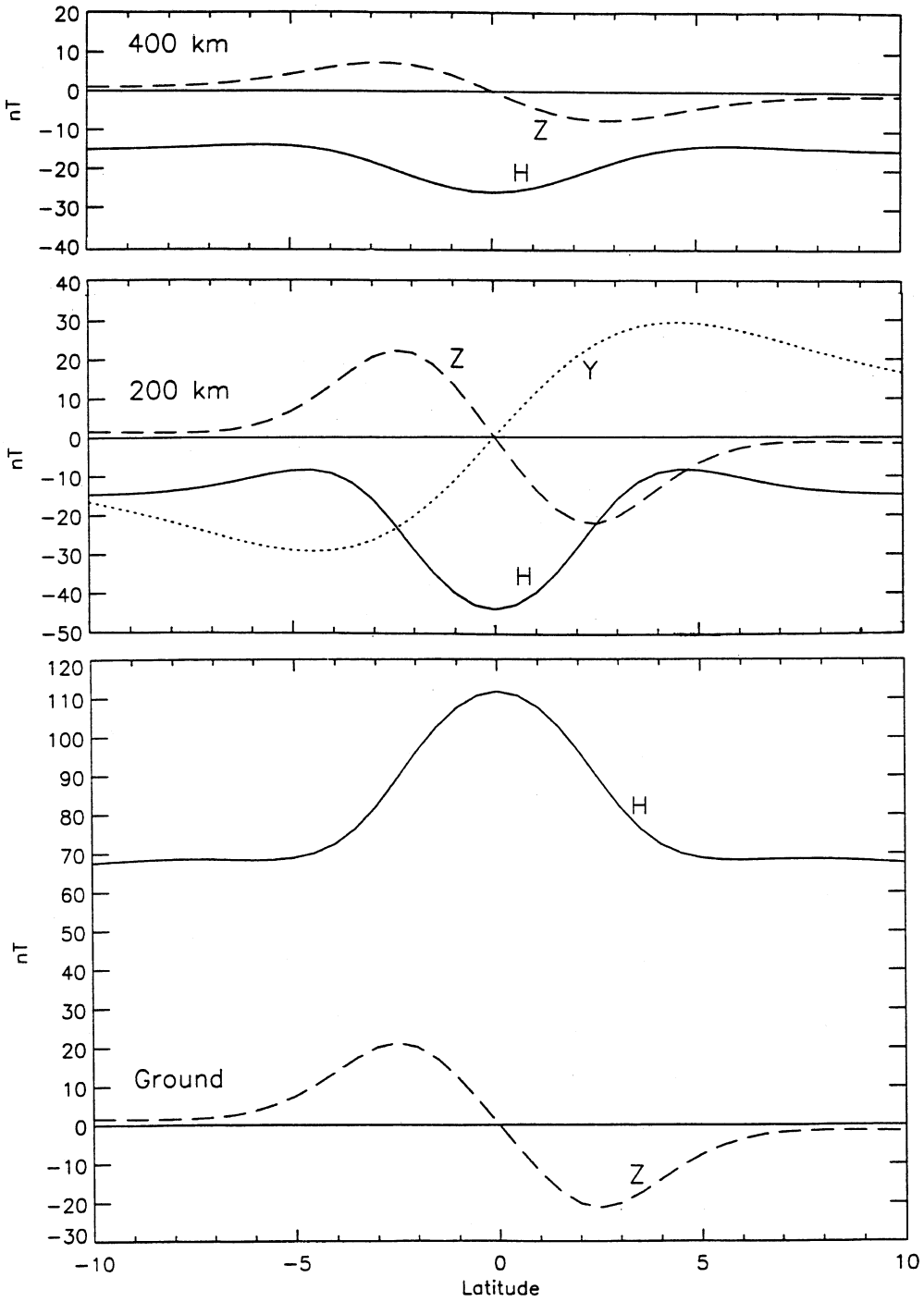

Fig. 4. Latitude distributions of magnetic perturbations at the ground (bottom), at 200 km (middle), and at 400 km (top) for the simulation including high-altitude westward winds. H = northward perturbation; Y = eastward perturbation; Z = downward perturbation. The Y variation is zero at the ground, and is non-zero but not calculated at 400 km.

ment to the background current.The Biot-Savart relation is applied to the electrojet supplemental current density, including image currents in the Earth that represent the effects of a perfectly conducting layer at 600 km depth.The background current sheet produces equal and opposite H perturbations above and below it, to which is added a constant value at all heights to represent the effects of an induced Earth current sheet. This constant value has 60% the magnitude of the magnetic perturbations that are produced directly by the infinite ionospheric current sheet. It enhances the magnetic effect of the background ionospheric current below the ionosphere, and reduces its effect above the ionosphere.

At the ground, the relative equatorial enhancement of H, with respect to H values at $\pm 10^{\circ}$ latitude, is less than what is obtained without winds (e.g. Richmond, 1973), because the wind profile used here tends to cause an increase in the eastward current at higher latitudes. With respect to the extrema of Z around $\pm 3^{\circ}$ latitude, the Z perturbation at higher latitudes is smaller for this simulation than for simulations without winds. There are no eastward magnetic perturbations at the ground, because they are confined within the current region itself in this two-dimensional model, analogous to the confinement of toroidal magnetic fields to altitudes where currents flow in a three-dimensional spherical terrestrial ionosphere.

At 400 km altitude, the H perturbation is weaker and its sign is reversed, since we are now farther from the eastward electrojet currents and above instead of below them. In addition, induced Earth currents act to reduce the H magnetic effects of the ionospheric currents above the ionosphere. Y perturbations are not calculated at 400 km, because they depend sensitively on the local winds and conductivities, and the ionospheric conductivities above 200 km are very crude in this model, being simply extrapolated upward from the calculated values at 200 km with an exponential decay. It can be expected that the amplitude of the Y perturbation should generally decrease with increasing height above 200 km, and be small at 400 km. Because of large solar-cycle variations of the high-altitude conductivity, there is a strong solar-cycle variation of east-west magnetic perturbations associated with the low-latitude meridional currents (Takeda and Maeda, 1983).

At 200 km, the H and Z perturbations have similar characteristics to those at 400 km, but are considerably stronger, because of the proximity to the main eastward current layer. The Y perturbations are of comparable amplitude. Qualitatively, they have a form similar to what was observed on the evening passes of MAGSAT (Maeda et al., 1982, 1985; Langel et al., 1993), but the sign is reversed, owing to the fact that the high-altitude wind that drives the meridional current is westward around midday, as in the present simulation, but eastward around dusk, as in the simulation of Takeda and Maeda (1983).

3. Low and middle latitudes

Models of the ionospheric wind dynamo have been reasonably successful at simulating the regular S_q magnetic perturbations (e.g. Forbes and Lindzen, 1976a; Takeda et al., 1986; Richmond and Roble, 1987; Takeda and Yamada, 1987). Panels (a) and (b) of Fig. 5, from Richmond and Roble (1987), show the distributions of the height-integrated horizontal ionospheric current density and of the vertical component of the field-aligned current density at 300 km altitude, from a simulation for solar minimum equinox conditions at 17 Universal Time (UT). The model uses distributions of thermospheric winds and ionospheric conductivities that are symmetric about

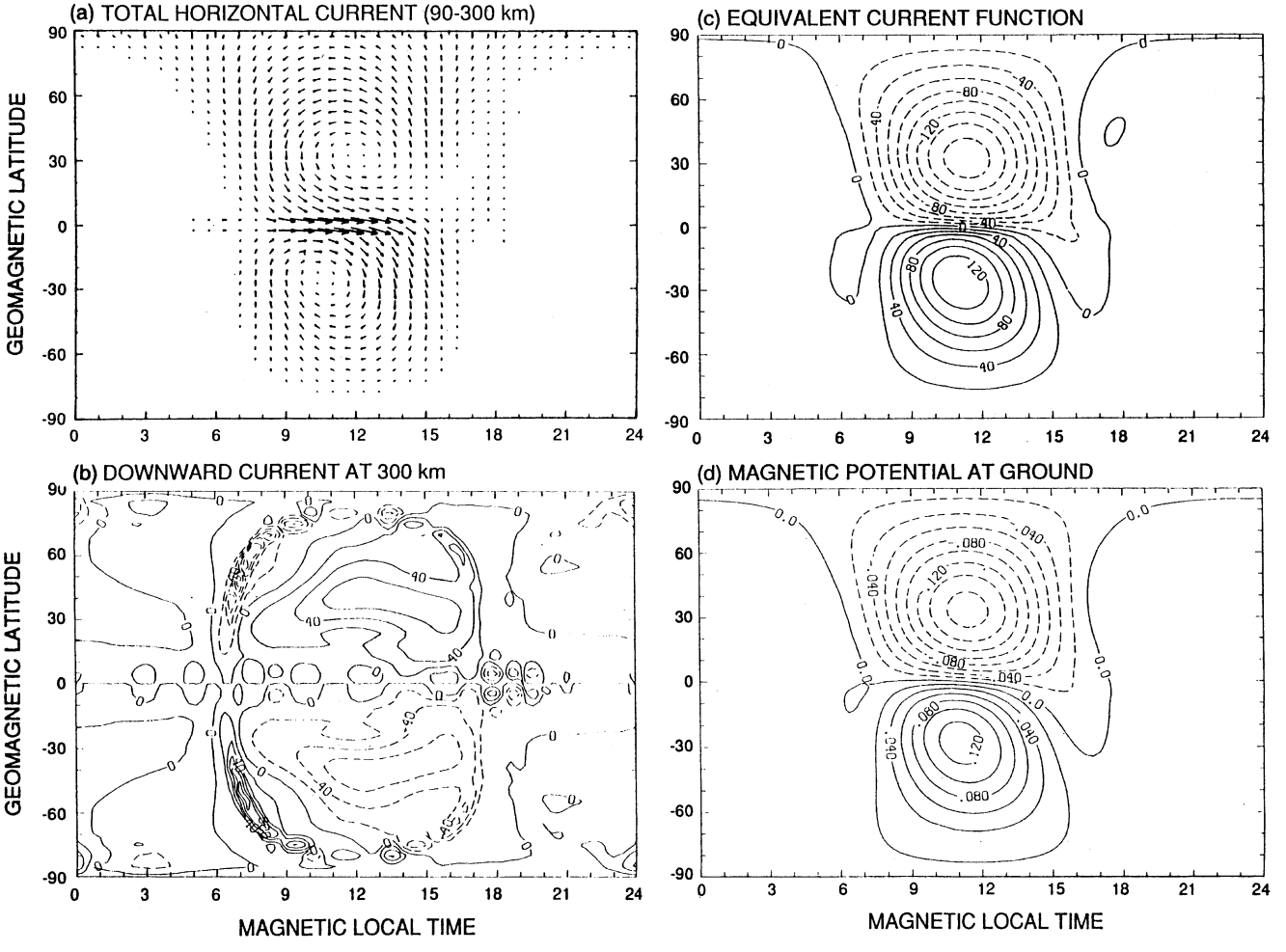

Fig. 5. Simulated ionospheric currents and their ground magnetic effects for solar-minimum equinox conditions, at 17 UT. (a) Total horizontal current flowing between 90 and 300 km. A vector equal in length to 1 h of magnetic local time represents 0.1 A/m. (b) Downward component of field-aligned current density at 300 km. The contour interval is 2 nA/m^2. Downward currents have solid contours; upward currents have dashed contours. (c) Equivalent current function for the entire three-dimensional current system in the ionosphere and above. The contour interval is 20 kA. (d) Magnetic perturbation potential at the ground, corresponding to the equivalent current in (c) plus effects of induced Earth currents. Magnetic perturbations are directed from high to low potentials. The contour interval is 0.02 T·m. [From Richmond and Roble (1987). Copyright by the American Geophysical Union.]

the geographic equator, but because its geomagnetic field is a tilted dipole, the winds and conductivities are asymmetric about the geomagnetic equator. At 17 UT the subsolar point lies about 11° north of the geomagnetic equator. In this simulation, net height-integrated ionospheric current flows southward across the geomagnetic equator, as seen in Fig. 5a, and it flows back to the northern hemisphere at midlatitudes along geomagnetic field lines, as evident from Fig. 5b. Near the dawn terminator in the southern hemisphere, some reversed downward field-aligned current flow is seen in Fig. 5b, which flows from the conjugate location in the northern hemisphere. The distribution of the field-aligned current flow is found to depend sensitively on the amount of asymmetry about the equator of the wind and conductivity distributions, so the patterns of field-aligned current flow in this example are not representative of other universal times or other seasons. The magnetic perturbations on the ground due to this entire three-dimensional current system are the same as those of the fictitious equivalent horizontal ionospheric current system shown in Fig. 5c. When an approximate effect of induced Earth currents corresponding to those induced in a magnetically impenetrable (perfectly conducting) layer at 600 km is added, the perturbation magnetic potential of Fig. 5d is obtained, whose negative gradient gives the horizontal components of the ground-level magnetic perturbations.

It can be expected that the effects of induced Earth currents will tend to reinforce the horizontal magnetic perturbations produced by the ionospheric currents at the ground, but to oppose the vertical perturbations. However, above the ionosphere the horizontal magnetic effects due to the ionospheric currents are reversed, and so the effects of the induced Earth current on them should generally tend to reduce their magnitude, as was found in the previous section for magnetic perturbations associated with the equatorial electrojet. Thus one might expect considerably smaller magnetic effects of S_q currents at LEO altitudes than at the ground. This would be a reasonable expectation if the Sq currents were limited to flow only in the ionosphere, without the field-aligned flow like that illustrated in Fig. 5b. However, some simple estimations of the total magnetic perturbations above the ionosphere, including the effects of the field-aligned current flow, show that S_q variations can be as large there as at the ground. Unlike the ground perturbations, these LEO S_q magnetic perturbations have a significant toroidal component.

Consider low latitudes around 14 magnetic local time (MLT), when the south-to-north field-aligned current flow at midlatitudes is greatest. At the magnetic equator, the negative eastward gradient of the magnetic potential in Fig. 5d yields an eastward ground magnetic perturbation of about 10 nT. From Fig. 5a we can see that the southward component of true height-integrated ionospheric current at this location is about 20 mA/m.The change in eastward magnetic perturbation across this current layer,calculated from Ampére's law, is about 25 nT, yielding an estimated 15 nT westward perturbation at the top of the ionosphere. This westward perturbation can be considered to arise from the fact that this location is within a large current loop that flows southward in the ionosphere below, and is closed by northward field-aligned current above. Because the physical size of this current loop is very large, extending to midlatitudes and to field lines with apexes 1 Earth radius or more above the Earth's surface, the toroidal magnetic perturbations associated with it extend over a large geographic region, not only in latitude but also in MLT and altitude. Furthermore, this particular simulation has a relatively modest amount of interhemispheric asymmetry, associated only with the 11° dipole tilt but excluding larger seasonal variations of the ionospheric conductivities and winds, and so we may expect that much larger toroidal magnetic effects at LEO altitudes exist for solstitial conditions, in association with larger

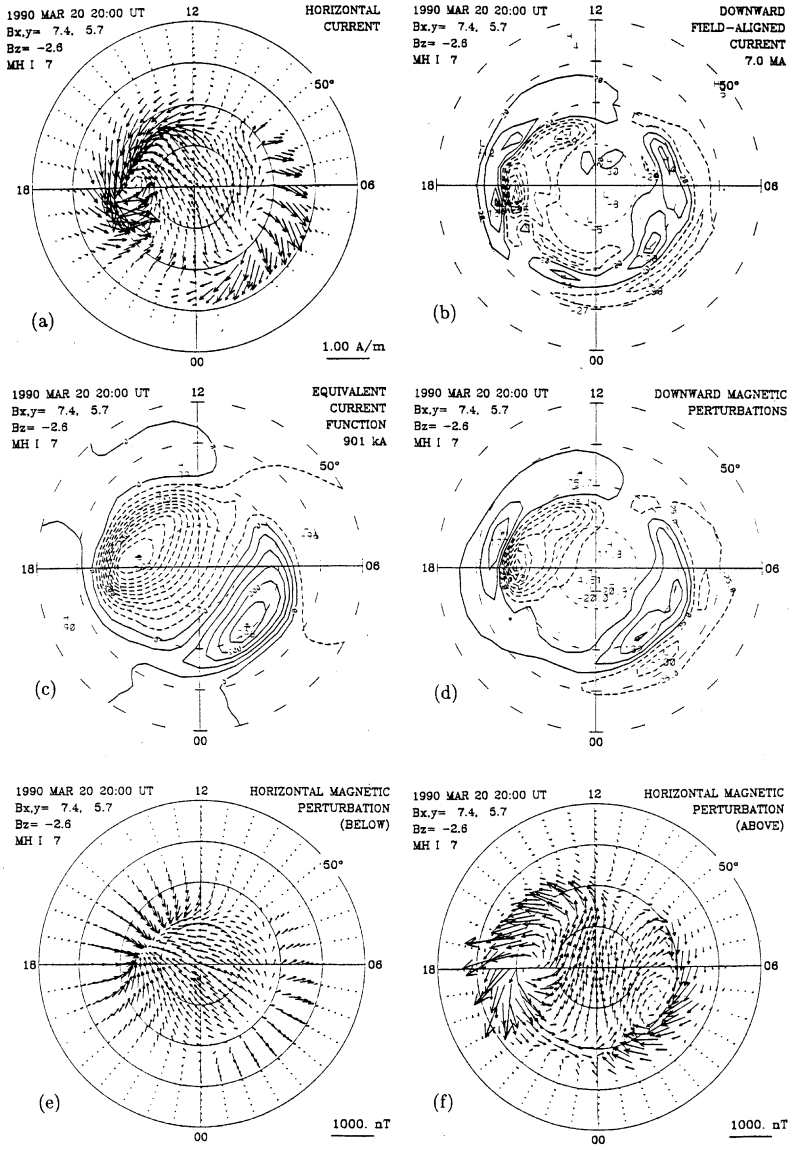

Fig. 6. Estimated ionospheric currents and associated magnetic effects in the northern magnetic hemisphere on 20 March 1990 at 20 UT. Coordinates are magnetic latitude, from 50° to the north magnetic pole, and MLT. The IMF (x, y, z) values are (7.4, 5.7, −2.6) nT, and the hemispheric power index is 7. (a) Height-integrated horizontal ionospheric electric current density. The vector scale is at the lower right. (b) Downward field-aligned current density at the top of the ionosphere. The contour interval is 400 nA/m^2, beginning at ±200 nA/m^2. Downward currents have solid contours; upward currents have dashed contours. (c) Equivalent current function, showing streamlines of toroidal ionospheric current. Equivalent current flows clockwise around the maximum (+) and counterclockwise around the minimum (−), with 50 kA between contours. (d) Vertical magnetic perturbations at the ground. The contour interval is 50 nT, beginning at ±25 nT. Downward perturbations have solid contours; upward perturbations have dashed contours. (e) Horizontal magnetic perturbations just below the ionospheric current sheet. The vector scale is at the lower right. (f) Horizontal magnetic perturbations just above the ionospheric current sheet.

field-aligned current flow. Because this flow is sensitive to the asymmetry of the thermospheric wind about the magnetic equator, LEO observations of the associated magnetic perturbations can potentially provide valuable information about the properties of the global winds that drive the ionospheric dynamo.

4. High latitudes

The largest field-aligned currents and associated toroidal magnetic perturbations occur at high magnetic latitudes. They are highly variable, and depend strongly on the direction and strength of the interplanetary magnetic field (IMF), as well as on other interplanetary and magnetospheric conditions. Fig. 6 shows patterns of the high-latitude northern-hemisphere electric currents and associated magnetic perturbations on 20 March 1990 at 20 UT, estimated with the assimilative mapping of ionospheric electrodynamics (AMIE) procedure (Richmond and Kamide, 1988), using a combination of ground magnetometer data and observations of ionospheric electric fields by radars and a satellite. The coordinates are magnetic latitude, above 50°, and MLT. This was a moderately active time, with IMF values of $B_x = 7.4$ nT, $B_y = 5.7$ nT, and $B_z = -2.6$ nT, in the orthogonal geocentric solar-magnetospheric coordinate system (x toward the Sun, z in the plane containing the x axis and the geomagnetic dipole axis, positive northward, and y completing the right-handed system). Auroral particle precipitation and the associated auroral enhancements in ionospheric conductivity were characterized by a hemispheric power index (Foster et al., 1986) of 7; this index was also used in the AMIE procedure to select an a priori statistical pattern of electric potential derived from Millstone Hill radar observations of ionospheric drifts (Foster et al., 1986).

The auroral electrojets, eastward in the afternoon and evening and westward in the early morning, show clearly in Fig. 6a. The typical patterns of downward and upward field-aligned currents above the ionosphere at the equatorward and poleward edges, respectively, of the eastward electrojet, and at the poleward and equatorward edges, respectively, of the westward electrojet, are apparent in Fig.6b.The total downward current, integrated over the hemisphere, is 7.0 MA,which equals the total integrated upward current.

For calculating the magnetic perturbations from the three-dimensional current system, the AMIE procedure uses three simplifying approximations: (a) the field-aligned currents are assumed to be precisely radial to the Earth; (b) the height-integrated horizontal ionospheric currents are assumed to flow in a thin current sheet at 110 km altitude; and (c) induced Earth current effects are calculated as those of a perfectly conducting layer at a depth of 250 km. (A perfect conductor at around this depth is able to represent a portion of the time-varying medium-scale induced auroral-zone magnetic perturbations (e.g. Richmond and Baumjohann, 1984). The current system is divided into a toroidal current in the ionospheric sheet layer, which produces poloidal magnetic perturbations, and a poloidal current consisting of the field-aligned currents and their closing irrotational currents in the ionospheric current sheet, which together produce toroidal magnetic perturbations above the ionosphere and zero perturbations below. The toroidal current can be represented by an equivalent current function, as shown in Fig. 6c. A total of 901 kA of equivalent current flows between the two points marked with a "+" and a "−", in the direction from late evening toward late morning.This is nearly an order of magnitude smaller than the total downward field-aligned current, as is typically the case (e.g. Richmond et al., 1990).

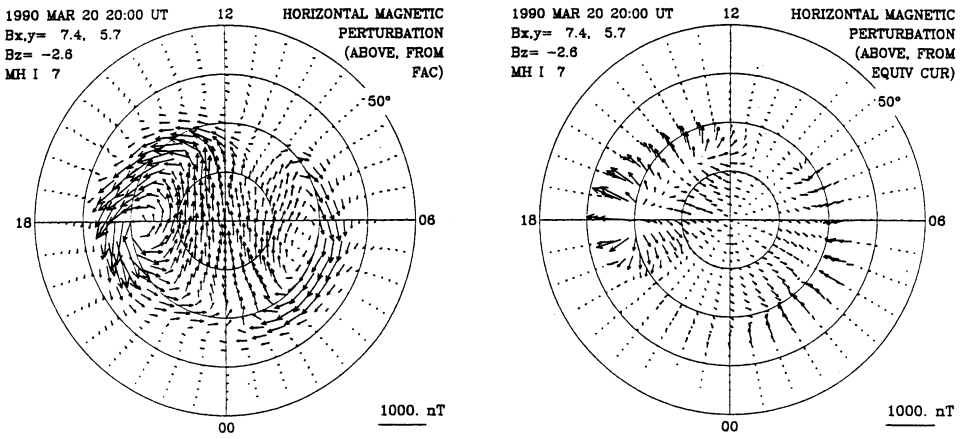

Fig. 7. Horizontal magnetic perturbations just above the ionospheric current sheet, corresponding to the toroidal (left) and poloidal (right) components of the total perturbations shown in Fig. 6f.

The equivalent current, together with the effects of the induced Earth currents, is responsible for the vertical magnetic variations. These are shown at ground level in Fig. 6d; they increase in strength somewhat with altitude up to the height of the ionospheric current layer, and then decrease above that in a manner analogous to the Z variations associated with the equatorial electrojet (Fig. 4). The horizontal magnetic perturbations in Figs. 6e,f are calculated immediately below and above the current layer at 110 km. Fig. 7 shows the components of the horizontal magnetic perturbations at the top of the current layer that are associated separately with the field-aligned currents (FAC, and their closing irrotational currents in the current sheet) and with the equivalent current (plus the induced Earth currents).

Note that the poloidal magnetic perturbations (associated with the toroidal equivalent current) decrease in strength with increasing altitude above the ionosphere, in a manner analogous to the H and Z equatorial-electrojet perturbations above the ionosphere shown in Fig. 4, so that at 400 km or above they are considerably weaker than those shown on the right in Fig. 7. In contrast, the toroidal magnetic perturbations associated with the field-aligned currents, shown on the left of Fig. 7, are relatively large at the top of the ionospheric current layer, and have amplitudes that decrease only slowly with increasing altitude. They therefore will tend to dominate the magnetic signatures of the currents at LEO altitudes above 400 km or so. Thus LEO observations of the magnetic perturbations give important information about the distributions of field-aligned currents, which in turn provide valuable information about the electromagnetic energy transfer from the magnetosphere to the ionosphere (e.g. Rich et al., 1987). Even low-precision LEO magnetic measurements, when carefully processed, provide useful information, particularly if a large number of simultaneous observations exists (e.g. Anderson et al., 2000).

5. Conclusions

This brief survey of some models of the magnetic perturbations produced by ionospheric and field-aligned currents has illustrated the significantly different character of the perturbations at

the ground from those at LEO altitudes. In particular, poloidal currents that produce no magnetic perturbations at the ground can have a major influence on the perturbations at LEO altitudes, at all latitudes. As a consequence, LEO observations of the magnetic perturbations can provide much valuable additional information about the properties of ionospheric currents, beyond what ground magnetic data can yield. This information can help us better understand the physical mechanisms that drive the currents.

Within a few degrees of the magnetic equator during the day, both at the ground and up to a few hundred kilometers above the ionosphere, magnetic perturbations tend to be dominated by the equatorial electrojet.The strength of this depends on both the ionospheric conductivity and the strength of the eastward ionospheric electric field at the equator, which itself responds to the global ionospheric dynamo. Several degrees off the equator the ionospheric currents are strongly influenced by east–west thermospheric winds, in addition to the east–west electric field. Poloidal currents in the upper equatorial ionosphere are also strongly influenced by east–west winds there. These poloidal currents can create significant east–west magnetic perturbations in the upper ionosphere.

Field-aligned S_q currents flowing between the northern and southern magnetic hemispheres can produce significant large-scale magnetic perturbations at LEO altitudes and at middle and low latitudes. These currents and their associated magnetic perturbations are sensitive to asymmetry about the magnetic equator of the distributions of the ionospheric conductivities and thermospheric winds that drive the ionospheric dynamo.

Electric currents in the auroral zones and the geomagnetic-field-aligned currents that connect into them generally produce larger magnetic perturbations than do the equatorial and mid-latitude currents. The character of these perturbations is very different below and above the ionospheric current layer, and tends to be dominated by toroidal magnetic perturbation fields associated with the field-aligned currents at LEO altitudes. Observations of these perturbations can provide valuable information about the state of the magnetosphere and about the transfer of energy between the magnetosphere and the ionosphere.

Acknowledgements

I thank Delores Knipp and Barbara Emery for helping to carry out the AMIE analysis of ionospheric electric fields and currents for the example presented in this paper, and Gang Lu for helpful comments. This work was supported in part by the NASA Sun-Earth Connection Theory and Supporting Research and Technology Programs.

References

Anandarao, B.G., Raghavarao, R., 1987. Structural changes in the currents and fields of the equatorial electrojet due to zonal and meridional winds. J. Geophys. Res. 92, 2514–2526.

Anderson, B.J., Takahashi, K., Toth, B.A., 2000. Sensing global Birkeland currents with Iridium engineering magnetometer data. Geophys. Res. Lett. 27, 4045–4048.

Fambitakoye, O., Mayaud, P.N., Richmond, A.D., 1976. Equatorial electrojet and regular daily variation S_R, III. Comparison of observations with a physical model. J. Atmos. Terr. Phys. 38, 113–121.

Forbes, J.M., Lindzen, R.S., 1976a. Atmospheric solar tides and their electrodynamic effects—I. The global Sq current system. J. Atmos. Terr. Phys. 38, 897–910.

Forbes, J.M., Lindzen, R.S., 1976b. Atmospheric solar tides and their electrodynamic effects- II. The equatorial electrojet. J. Atmos. Terr. Phys. 38, 911–920.

Foster, J.C., Holt, J.M., Musgrove, R.G., Evans, D.S., 1986. Ionospheric convection associated with discrete levels of particle precipitation. Geophys. Res. Lett. 13, 656–659.

Gagnepain, J., Crochet, M., Richmond, A.D., 1977. Comparison of equatorial electrojet models. J. Atmos. Terr. Phys. 39, 1119–1124.

Hedin, A.E., Biondi, M.A., Burnside, R.G., Hernandez, G., Johnson, R.M., Killeen, T.L., Mazaudier, C., Meriwether, J.W., Salah, J.E., Sica, R.J., Smith, R.W., Spencer, N.W., Wickwar, V.B., Virdi, T.S., 1991. Revised global model of thermospheric winds using satellite and ground-based observations. J. Geophys. Res. 96, 7657–7688.

Langel, R.A., Purucker, M., Rajaram, M., 1993. The equatorial electrojet and associated currents as seen in Magsat data. J. Atmos. Terr. Phys. 55, 1233–1269.

Maeda, H., Iyemori, T., Araki, T., Kamei, T., 1982. New evidence of a meridional current system in the equatorial ionosphere. Geophys. Res. Lett. 9, 337–340.

Maeda, H., Kamei, T., Iyemori, T., Araki, T., 1985. Geomagnetic perturbations at low latitudes observed by MAGSAT. J. Geophys. Res. 90, 2481–2486.

Rich, F.J., Gussenhoven, M.S., Greenspan, M.E., 1987. Using simultaneous particle and field observations on a low altitude satellite to estimate Joule heat energy flow into the high latitude ionosphere. Ann. Geophysicae 5A, 527–534.

Richmond, A.D., 1973. Equatorial electrojet—I. Development of a model including winds and instabilities. J. Atmos. Terr. Phys 35, 1083–1103.

Richmond, A.D., Baumjohann, W., 1984. Three-dimensional analysis of magnetometer array data. J. Geophys. 54, 138–156.

Richmond, A.D., Kamide, Y., 1988. Mapping electrodynamic features of the high-latitude ionosphere from localized observations: Technique. J. Geophys. Res. 93, 5741–5759.

Richmond, A.D., Roble, R.G., 1987. Electrodynamic effects of thermospheric winds from the NCAR Thermospheric General Circulation Model. J. Geophys. Res. 92, 12365–12376.

Richmond, A.D., Thayer, J.P., 2000. Ionospheric electrodynamics: a tutorial. In: Lysak, R.L., Hesse, M., Fujii, R., Ohtani, S. (Eds.), Magnetospheric Current Systems. Am. Geophys. Union, Washington DC, pp. 131–146.

Richmond, A.D., Kamide, Y., Akasofu, S.-I., Alcaydé Blanc, M., de la Beaujardiére, O., Evans, D.S., Foster, J.C., Friis-Christensen, E., Holt, J.M., Pellinen, R.J., Senior, C., Zaitzev, A.N., 1990. Global measures of ionospheric electrodynamic activity inferred from combined incoherent scatter radar and ground magnetometer observations. J. Geophys. Res. 95, 1061–1071.

Stening, R.J., 1985. Modeling the equatorial electrojet. J. Geophys. Res. 90, 1705–1719.

Takeda, M., Araki, T., 1985. Electric conductivity of the ionosphere and nocturnal currents. J. Atmos. Terr. Phys 47, 601–609.

Takeda, M., Maeda, H., 1983. F-region dynamo in the evening—interpretation of equatorial ΔD anomaly found by MAGSAT. J. Atmos. Terr. Phys. 45, 401–408.

Takeda, M., Yamada, Y., 1987. Simulation of ionospheric electric fields and geomagnetic field variation by the ionospheric dynamo for different solar activity. Ann. Geophysicae 5A, 429–434.

Takeda, M., Yamada, Y., Araki, T., 1986. Simulation of ionospheric currents and geomagnetic field variations of S_q for different solar activity. J. Atmos. Terr. Phys. 48, 277–287.

Untiedt, J., 1967. A model of the equatorial electrojet involving meridional currents. J. Geophys. Res. 72, 5799–5810.